Non-framework Coordination Polymers With Tunable Bimodal Porosities Based on Inter-connected Metal-organic Polyhedra

Heejin Jung, Dohyun Moon,[†,*] and Hyungphil Chun[*]

Department of Applied Chemistry, College of Science and Technology, Hanyang University, Ansan 426-791, Korea
[*]E-mail: hchun@hanyang.ac.kr
[†]Beamline Division, Pohang Accelerator Laboratory, Pohang, Kyungbuk 790-784, Korea. [*]E-mail: dmoon@postech.ac.kr

One discerns coordination polymers (CPs) and metal-organic frameworks (MOFs) because the former provides a more comprehensive concept for network solids based on metal ions and multitopic organic ligands, while the latter implies the presence of a crystal lattice in the structure.[1] MOF materials with three-dimensional backbones and well-defined network structures possess many advantages compared to their non-framework analogues, such as homogeneous and reproducible material properties, and atom-level information on the structures. However, the labile nature of some coordination bonds, such as those between first-row transition elements and carboxylate ligands may lead to a gradual or even complete degradation of the scaffold under ambient conditions.[2] For most MOFs, therefore, the sustainability of the crystal lattice is a prerequisite to realize the fascinating potentials[3] of these materials, including hydrogen storage or carbon capture and sequestration.[4] Consequently, it is desirable to have a new type of materials that possess the advantages of porous MOFs but without the constraint of an ordered crystal lattice. Approaches taken in this direction include polymerizations using rigid building blocks such as phthalocyanins,[5] liquid-crystal templation[6] and the derivation of disordered structures using rapid precipitation methods.[7]
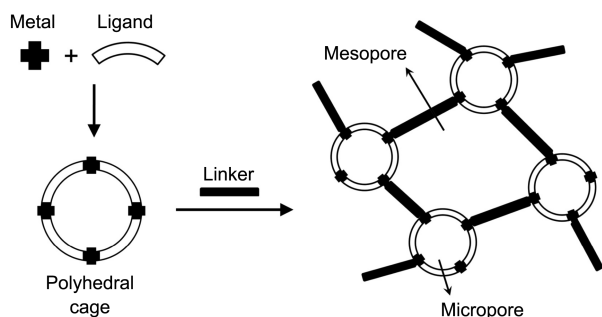
We provide a potential alternative in another perspective, and hereby report some examples of non-framework CPs that have intrinsic porosities tunable between microporous and mesoporous regimes. The idea is based on the realization that some of the well-known metal-organic polyhedral cages are equipped with solvent-coordinated sites.[8] Cu_2 paddlewheels and bent dicarboxylates are prototypical building blocks for such cases. Thus we decided to take advantage of the solvent sites of paddlewheel units to cross-link polyhedral cage molecules into a network.[9] The polymeric materials would possess a mesoporosity depending on the size of the cage and linker molecules, as well as an intrinsic microporosity originating from the inner cage voids (Scheme 1).

We used 2,7-naphthalenedicarboxylate and Cu^{2+} to build a macromolecule with 12 Cu_2 paddlewheel units, $[Cu_{24}(2,7\text{-}ndc)_{24}(DMF)_{10}(H_2O)_{14}]$ (**1**). The structure of the cuboctahedral cage molecule was determined by X-ray crystallography on weakly diffracting single-crystals using synchrotron X-rays from Pohang Accelerator Laboratory, Korea (Figure 1).[10]

The approximately spherical molecule measures about 3.3 nm, and the inner-cage void can host an imaginary sphere with the diameter of 1.8 nm. Such metal-organic cuboctahedra were first reported by Yaghi[11] and Zaworotko,[12] and continue to be a subject of active research.[13]

In the packing structure, a given cuboctahedral cage

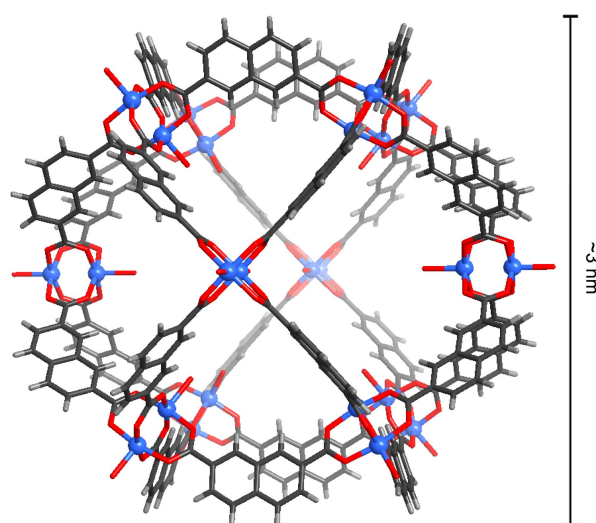**Scheme 1.** Stepwise synthesis of non-framework coordination polymers having a bimodal porosity.

Figure 1. Structure of the cuboctahedral cage molecule of **1** determined by X-ray crystallography. The triangular and square windows have the free passages of 5.4 and 8.4 Å, respectively.

Figure 2. Simulated and experimental X-ray powder diffraction patterns for **1**.

makes close contacts with neighbors through its 8 triangular windows, and consequently **1** adopts a body-centered cubic (bcc) packing structure where the coordination number is 8 (Fig. S3). The overall structure of **1** is further characterized by the solvent-accessible voids of 22147 Å^3 per unit cell or 68% of the total crystal volume.[14]

X-ray powder diffraction (XRPD) studies show that the crystal structure of **1** shown in Figure 1 represents the bulk product (Fig. 2).

When **1** is solvent-exchanged and evacuated under a dynamic vacuum, a complete amorphization occurs as evidenced by the disappearance of the Bragg diffractions in the XRD patterns. The amorphization, however, is not an indication of irreversible decomposition of the cage molecules, but simply a collapse of the bcc packing resulting from the removal of space-filling solvent molecules. The reversible uptake and release of gas molecules by amorphized **1** is the evidence.

As shown in Figure 3 and 4, the sorptions of N_2 (77 K), CO_2 (195 K) and H_2 (77 K) by **1** show reversible type I

Figure 3. N_2 sorption isotherms measured at 77 K for **1-4**. Filled and open symbols denote adsorption and desorption, respectively.

Figure 4. CO_2 and H_2 sorption isotherms for **1-4** measured at 195 and 77 K, respectively.

isotherms without a notable hysteresis. The BET and Langmuir surface areas determined from the N_2 sorption data are 610 and 800 m^2/g, respectively. The total pore volume is 0.287 cm^3/g and is significantly lower than the solvent-accessible voids estimated from the crystal structure. This is because only the intracage voids are available for gas adsorption in amorphized **1**. Note that the pore volume estimated only from the intracage voids is close at 0.261 cm^3/g assuming the crystallographic density of the sample.

With the 'permanently' porous molecular solids in hand, we then used various diamine ligands in order to cross-link the cage molecules into a series of non-framework CPs (Scheme 2).

This was readily done by slowly adding a diluted solution of diamine into the slurry or solution of **1**. Three such materials have been obtained where the linkers are short (ethylenediamine, en), rigid aromatic (xylenediamine, xn) or flexible (diaminoheptane, hn) diamine ligands for **2**, **3** and **4**, respectively. The incorporation of the diamine spacers leads to the color change of the samples from green to blue, and was confirmed by the appearance of sharp NH stretching bands at 3310, 3314 and 3306 cm^{-1} for **2-4**, respectively, in

Scheme 2. Preparation of non-framework coordination polymers **2-4** from polyhedral cage **1** and diamine linkers.

IR spectroscopy (Fig. S1). In thermal gravimetric analysis of the three CPs, the solvent contents are significantly reduced, and the weight for non-volatile organic residues are much increased compared to **1** (Fig. S2). It was not possible to quantify the exact number of the diamine linkers per cage unit in **2-4**; however, the increased N contents in the elemental analysis suggest that most of the external solvent sites are occupied by the diamine ligands (see Supporting Information for details). XRPD analysis on **2-4** shows that **2** possesses a considerable crystallinity while **3** and, especially **4** are mostly amorphous (Fig. S4).

The N_2 sorption isotherms of **2-4** indicate that the three CPs possess surface features clearly distinct from that of **1** which is a typical microporous solids (Fig. 3).

First, the early uptake at $P/P_0 < 0.05$ is gradually lowered on going from **2** to **4**, which indicates decreasing micropores, i.e., cuboctahedral cages, in a unit weight of the sample. Instead, **2-4** display unusual type II isotherms due to unrestricted monolayer-multilayer adsorptions at $P/P_0 \sim 1$, and large hysteresis loops characteristic of mesoporous materials. The trends in the N_2 sorption data corroborate with the changes in the spacer ligands in the following way. When the large cage molecules are interconnected by short spacers (en in **2**), it would give slit-type intercage voids while most of the pores are still in the microporous region (< 2 nm). This results in the narrow hysteresis for **2** which is a type H4 according to the IUPAC classification.[15] When relatively long linkers connect the cage molecules (xn for **3** and hn for **4**), mesopore volumes increase substantially to give the large hysteresis loops related to pore condensations. Finally, the desorption branch of the isotherm for **4** shows the hysteresis step less steeper than that of **3** implying a much broader pore size distribution for **4** (Fig. S9). This is because hn is considerably more flexible than xn.

The sorption capacities for CO_2 at 195 K and 1 bar are systematically lowered on going from purely microporous **1** to rather mesoporous **4** (Fig. 4), and this is in accordance with the decrease in the micropore volumes.[16]

This result is not surprising because the adsorption of small gases is favored in micropores in which adsorption potentials from opposite walls overlap giving strong fluid-wall interactions.[17] The isosteric heats (Q_{ST}) of CO_2 adsorption calculated using the Virial-type equations[18] for **2** and **3** are slightly lower than that for **1** which is 30 kJ/mol (Fig. S9). These values are somewhat higher than those reported for three representative ZIFs.[19] For comparison, microporous zeolites have Q_{ST} values in the range 30-45 kJ/mol depending on the channel structure and cations,[20] and the mesoporous material MCM-41 has been reported to have 25 kJ/mol.[21]

The sorptions of CO_2 at 273 K (Fig. S5) and H_2 at 77 K (Fig. 4) also show a gradual decrease for **1-4**, but the lack of strong intermolecular interactions between adsorptive molecules results in much pronounced drops in the sorption capacities for **3** and **4** compared to **1** and **2**. Again, this proves that microporous materials are advantageous over mesoporous materials in terms of gas storage through physi-sorption.

The poor performances of **2-4** in the uptake of H_2 and CO_2 do not disapprove our approaches towards new materials based on non-framework CPs. This is in part because there are much room for modulating the basic building blocks, and in part because the absolute sorption capacity is not the sole target in the design of these materials. Also, non-framework CPs with an intrinsic porosity may be used for other purposes such as a support for loading catalysts or nano-materials in heterogeneous host-guest chemistry.[22]

In conclusion, we have shown that it is possible to synthesize and systematically modulate intrinsic bimodal porosities of non-framework CPs. The porosities of these materials may be tuned by the judicious choice of the cage molecules and the linkers, and therefore this type of materials is potentially useful adsorbents when a bimodal porosity is required. The absence of an ordered crystal lattice in the structure of these porous materials is an advantage over conventional MOFs. The open metal sites and nano-meter-sized cages may also be useful for loading functional guest molecules.

Supplementary Materials. Details of the synthesis, thermogravimetric analysis, spectroscopic data, gas sorption analysis for **1-4**, X-ray powder diffraction patterns for **2** and **3**, and crystallographic data in CIF format for **1**.

References

1. For a more detailed account on the terminologies, see Biradha, K.; Ramanan, A.; Vittal, J. J. *Cryst. Growth Des.* **2009**, *9*, 2969.
2. Low, J. J.; Benin, A. I.; Jakubczak, P.; Abrahamian, J. F.; Faheem, S. A.; Willis, R. R. *J. Am. Chem. Soc.* **2009**, *131*, 15834.
3. (a) Horike, S.; Shimomura, S.; Kitagawa, S. *Nature Chem.* **2009**, *1*, 695. (b) Kuppler, R. J.; Timmons, D. J.; Fang, Q.-R.; Li, J.-R.; Makal, T. A.; Young, M. D.; Yuan, D.; Zhao, D.; Zhuang, W.; Zhou, H.-C. *Coord. Chem. Rev.* **2009**, *253*, 3042. (c) Lee, J.; Farha, O. K.; Roberts, J.; Scheidt, K. A.; Nguyen, S. T.; Hupp, J. T. *Chem. Soc. Rev.* **2009**, *38*, 1450. (d) Czaja, A. U.; Trukhan, N.; Mller, U. *Chem. Soc. Rev.* **2009**, *38*, 1284. (e) Suh, M. P.; Cheon, Y. E.; Lee, E. Y. *Coord. Chem. Rev.* **2008**, *252*, 1007. (f) Frey, G. *Chem. Soc. Rev.* **2008**, *37*, 191. (g) Maspoch, D.; Ruiz-Molina, D.; Veciana, J. *Chem. Soc. Rev.* **2007**, *36*, 770.
4. (a) Phan, A.; Doonan, C. J.; Uribe-Romo, F. J.; Knobler, C. B.; O'Keeffe, M.; Yaghi, O. M. *Acc. Chem. Res.* **2010**, *43*, 58. (b) Haszeldine, R. S. *Science* **2009**, *325*, 1647. (c) Murray, L. J.; Dinca, M.; Long, J. R. *Chem. Soc. Rev.* **2009**, *38*, 1294. (d) Thomas, K. M. *Dalton Trans.* **2009**, 1487. (e) Morris, R. E.; Wheatley, P. S. *Angew. Chem. Int. Ed.* **2008**, *47*, 4966.
5. McKeown, N. B.; Budd, P. M.; Msayib, K. J.; Ghanem, B. S.; Kingston, H. J.; Tattershall, C. E.; Makhseed, S.; Reynolds, K. J.; Fritsch, D. *Chem. Eur. J.* **2005**, *11*, 2610.
6. Roy, X.; MacLachlan, M. J. *Chem. Eur. J.* **2009**, *15*, 6552.
7. Xin, Z.; Bai, J.; Shen, Y.; Pan, Y. *Cryst. Growth Des.* **2010**, *10*,

2451.

8. Tranchemontagne, D. J.; Ni, Z.; O'Keeffe, M.; Yaghi, O. M. *Angew. Chem. Int. Ed.* **2008**, *47*, 5139.

9. A similar attempt to crosslink polyhedral molecules through the derivatization of dicarboxylate ligand has been reported. See Tonigold, M.; Hitzbleck, J.; Bahnmller, S.; Langstein, G.; Volkmer, D. *Dalton Trans*. **2009**, 1363.

10. Almost the same compound, [$Cu_{24}(2,7\text{-}ndc)_{24}\cdot(DEF)_8(H_2O)_{16}$], has been reported by Yaghi and coworkers that crystallizes in an orthorhombic space group. However, the gas sorption property of the metal-organic polyhedra has not been reported. See Furukawa, H.; Kim, J.; Ockwig, N. W.; O'Keeffe, M.; Yaghi, O. M. *J. Am. Chem. Soc*. **2008**, *130*, 11650.

11. Eddaoudi, M.; Kim, J.; Wachter, J. B.; Chae, H. K.; O'Keeffe, M.; Yaghi, O. M. *J. Am. Chem. Soc.* **2001**, *123*, 4368.

12. Moulton, B.; Lu, J.; Mondal, A.; Zaworotko, M. J. *Chem. Commun.* **2001**, 863.

13. (a) Perry, J. J., IV.; Perman, J. A.; Zaworotko, M. J. *Chem. Soc. Rev.* **2009**, *38*, 1400. (b) Prakash, M. J.; Lah, M. S. *Chem. Commun.* **2009**, 3326.

14. Spek, A. L. *PLATON, A Multipurpose Crystallographic Tool*; Utrecht University: Utrecht, The Netherlands, 2001.

15. Sing, K. S. W.; Everett, D. H.; Haul, R. A. W.; Moscou, L.; Pierotti, R. A.; Rouqurol, J.; Siemieniewska, T. *Pure Appl. Chem.* **1985**, *57*, 603.

16. 0.287, 0.222, 0.145 and 0.076 cm^3/g for **1-4**, respectively.

17. Lowell, S.; Shields, J. E.; Thomas, M. A.; Thommes M. in *Characterization of Porous Solids and Powders: Surface Area, Pore Size and Density*; Kluwer Academic Publishers: The Netherlands, 2004; pp 11-12.

18. Czepirski, L.; Jagieo, J. *Chem. Eng. Sci.* **1989**, *44*, 797.

19. Prez-Pellitero, J.; Amrouche, H.; Siperstein, F. R.; Pirngruber, G.; Nieto-Draghi, C.; Chaplais, G.; Simon-Masseron, A.; Bazer-Bachi, D.; Peralta, D.; Bats, N. *Chem. Eur. J.* **2010**, *16*, 1560.

20. (a) Shao, W.; Zhang, L.; Li, L.; *Adsorption* **2009**, *15*, 497. (b) Zukal, A.; Pawlesa, J.; Cejka, J. *Adsorption* **2009**, *15*, 264. (c) Joshi, P. N.; Shiralkar, V. P. *J. Phys. Chem.* **1993**, *97*, 619.

21. He, Y.; Seaton, N. A. *Langmuir* **2006**, *22*, 1150.

22. (a) Park, Y. K.; Choi, S. B.; Nam, H. J.; Jung, D.-Y.; Ahn, H. C.; Choi, K.; Furukawa, H.; Kim, J. *Chem. Commun.* **2010**, *46*, 3086. (b) Pan, Y.; Yuan, B.; Li, Y.; He, D. *Chem. Commun.* **2010**, *46*, 2280. (c) Witham, C. A.; Huang, W.; Tsung, C.-K.; Kuhn, J. N.; Somorjai, G. A.; Toste, F. D. *Nature Chem.* **2010**, *2*, 36.